



Marine Optics and Ocean Color Remote Sensing

Veloisa Mascarenhas and Therese Keck

Abstract

Light plays an important role in aquatic ecosystems, both marine and freshwater. Penetration of light underwater influences various biogeochemical processes and also influences activities and behavioral patterns of marine organisms. In addition, dissolved and particulate water constituents present in the water column absorb and scatter light, giving water its characteristic color. The concentration or abundance of these constituents, referred to as optically active constituents (OACs) also determine light availability underwater. Thus color being an indicator of water column content, serves as a water quality parameter. Monitoring of the ocean color variables, such as the OAC concentrations and their optical properties, therefore, allows assessment of the health of an ecosystem. Advances in optical methodologies have improved the understanding of our ecosystems through multispectral and hyperspectral in situ measurements and observations. However, the ocean environment is vast and dynamic and so limitations of spatial and temporal coverage have been overcome with satellite remote sensing that provides oceanographers with repeated synoptic coverage. Being recognized as an essential climate variable (ECV) ocean color is monitored as part of the climate change initiative (CCI) of the European Space Agency (ESA). This chapter aims to provide the reader with an overview of the science of ocean color, introducing involved common terminologies and concepts and its global coverage using satellite remote sensing.

V. Mascarenhas (✉)
Institut für Chemie und Biologie des Meeres, Universität
Oldenburg, Wilhelmshaven, Germany
e-mail: veloisa.john.mascarenhas@uni-oldenburg.de

T. Keck
Institute for Space Sciences, Freie Universität Berlin,
Berlin, Germany
e-mail: therese.keck@wew.fu-berlin.de

Introduction to Ocean Color, Fundamental Concepts, and Optical Tools

Veloisa Mascarenhas

Role of Light in Water

Sunlight plays a key role in the ecology of aquatic ecosystems. Its interaction with water, dissolved and particulate suspended materials is an important physical phenomenon and influences several biogeochemical processes in the global ocean. Penetration of sunlight below water surface facilitates associated biological processes like primary production or plankton distribution in the water column (Kirk 1994). In addition to facilitating photosynthetic processes which form the base of ecological food chain, sunlight also influences the behavioral patterns and activities of marine organisms which are affected by the ambient light field that undergoes vertical changes within the water column (Frank et al. 2012). Mesopelagic fish and zooplankton abundances in different coastal locations are known to correlate with light availability (Aksnes et al. 2004) and changes in light availability conditions are in turn known to have implications for mesopelagic regime shifts (Aksnes et al. 2009).

Fate of Light in Water: Optically Active Constituents and Optical Properties

Fresh and marine waters are a witch's brew of dissolved and particulate matter, both organic and inorganic (Mobley 1994). The dissolved and particulate materials in addition to water molecules interact with light and are therefore known as optically active constituents (OACs). Phytoplankton, colored dissolved organic matter (CDOM), and suspended particulate matter (SPM) being variable in time and space are the three OACs extensively studied across fresh and marine water eco-

systems (Binding et al. 2008; Garaba et al. 2014; Holinde and Zielinski 2016; Mascarenhas et al. 2017). The OACs in the medium interact with the ambient light via processes of absorption and scattering, which gives water its characteristic color. The processes of absorption and scattering are referred to as inherent optical properties (IOPs) of water and depend solely on the OACs present in water. Spatial and temporal variability in the type and abundance of these OACs subsequently induces variability in the IOPs of water. In addition to the IOPs, water bodies are also characterized in terms of their apparent optical properties (AOPs). The AOPs depend both on the OACs and the incident light field.

Phytoplankton are drifting microscopic algae that photosynthesize and form the base of food webs in aquatic (marine and freshwater) ecosystems. Chlorophyll, a green pigment in the phytoplankton absorbs preferentially the blue and red wavelengths of the visible light spectra and reflects green. Therefore, oceans with high concentrations of phytoplankton appear in shades of blue-green depending on the type and density of the phytoplankton population (e.g., North Sea water during algal blooms in Fig. 1). Although small in size, these organisms cause large scale impacts. For example, it has been proposed that phytoplankton can steer Pacific tropical cyclones (Gnanadesikan et al. 2010). CDOM, the optically active component of the dissolved organic matter pool, absorbs UV light in the surface waters which is harmful for phytoplankton (Kirk 1994). However, phytoplankton also compete with CDOM for light in the shorter visible wavelength spectra. Also known as yellow substances, *gelvin*, or

gelbstoff, CDOM occurs naturally in aquatic environments primarily as a result of tannin-stained waters released from decaying detritus (Coble 2007). Waters comprising of high concentrations of CDOM range from yellow-green to brown (e.g., lake water with dead organic material in Fig. 1). Inorganic suspended matter (ISM), the inorganic component of the SPM, strongly scatters longer (red) wavelengths, thereby giving waters with high sediment concentrations a reddish-brown color (e.g., Wadden Sea in Fig. 1). Pure water, however, absorbs longer wavelength red light. Therefore, open ocean waters with very low concentrations of OACs appear blue (e.g., Atlantic Ocean and North Sea water in Fig. 1). Hence, the OACs influence light availability underwater and determine the color of the oceans (Fig. 1).

Sunlight at the ocean surface is partly reflected (governed by Snell's law and Fresnel equations), while the rest is transmitted through the water column. Underwater light is then either absorbed and/or scattered by water molecules and the OACs present in the water column. The backwards-scattered light then gives water its characteristic color and carries information of ocean constituents, which is captured by satellite sensors hundreds of kilometers above the earth's surface (see section "Space-borne remote sensing"). Detailed understanding of light interactions with the OACs of a medium and its propagation in the medium is fundamental to radiative transfer studies in aquatic ecosystems. Therefore, optical oceanography, i.e., the study of light interactions in the oceans, is vital in understanding the underwater light field, bio-optical relations, and related ecosystem dynamics.

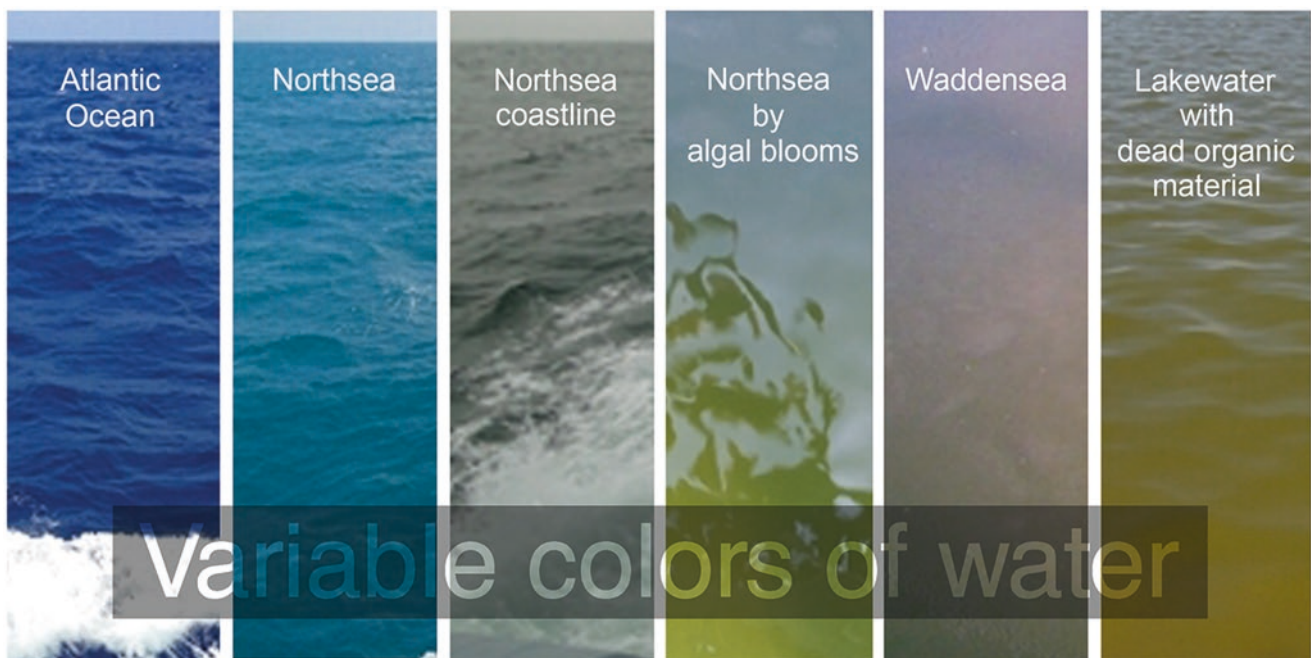


Fig. 1 Various colors observed in fresh and marine waters influenced by the presence of varying optically active constituents. (Reproduced with permission from Marcel Wernard, NIOZ)

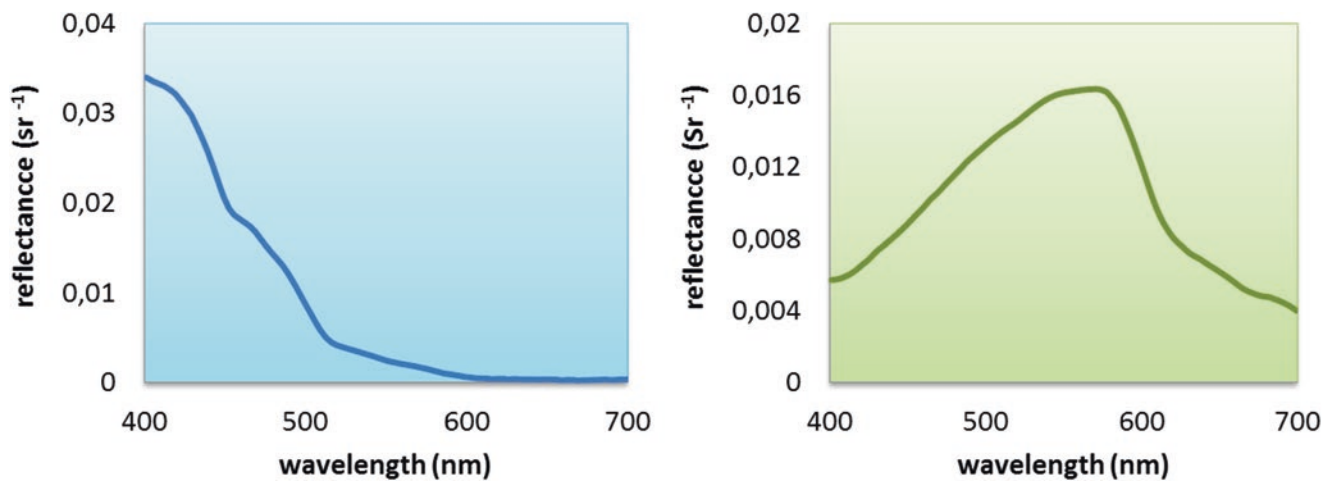


Fig. 2 Spectral reflectance in case-1 (Pacific Ocean) and case-2 waters (Norwegian Fjord). Case-1 waters consisting of very low optically active constituents (OACs), reflect light in the blue region. Case-2

waters with high concentrations of OACs (here chlorophyll *a* in phytoplankton), reflect strongly the green wavelengths. (Data: Daniela Voss, ICBM, University of Oldenburg)

In waters (mostly open ocean) consisting of very low phytoplankton abundances, most visible light is scattered by the water molecules. Water selectively scatters and absorbs certain wavelengths of visible light (Pope and Fry 1997). Longer wavelengths are quickly absorbed from water while shorter wavelengths penetrate deeper, which gives the deep open oceans their characteristic blue color (Fig. 2, blue spectra). In coastal waters (influenced by terrestrial runoff) with higher proportions of dissolved and particulate matter, both absorption and scattering increases, making them appear green (Fig. 2, green spectra) or brown depending on its constituents (Morel and Prieur 1977). Detailed and accurate understanding of the water constituents and their interaction with light is essential in studies of radiative transfer (Chang and Dickey 2004).

Light Penetration and Euphotic Depth

Only the surface layer of the ocean receives sufficient light to allow phytoplankton growth through primary production. Sunlight entering the ocean may travel up to 1000 m deep but there is barely any significant light beyond 200 m. Based on light availability, water columns are divided into 3 different zones. The upper 150–200 m layer of the ocean is called the ‘sunlit’ or the ‘euphotic’ zone. The extent of this layer is determined by the depth at which the Photosynthetically Active Radiation (PAR) reduces to 1% of its surface value. In bio-optical literature, PAR values are given in units of mol photons s⁻¹ m⁻² or einst s⁻¹ m⁻², where one einstein is one

mole of photons (6.023×10^{23} photons). PAR is a broadband quantity, often estimated using only the visible wavelengths, 400–700 nm (Mobley 1994). Beyond approximately 200 m depth, the intensity of light decreases rapidly with increasing depth and is insufficient to support any photosynthetic activity. From about 200–1000 m the zone is referred to as ‘twilight’ or ‘dysphotic’. Below 1000 m the zone is known as ‘aphotic’ or ‘midnight’ zone and is entirely dark.

The depth of the euphotic zone (*Z_{eu}*) depends highly on the turbidity of the water column caused by varying concentrations of organic and inorganic optically active constituents (OACs) present either in dissolved form or in suspension. Phytoplankton populations, dead organic matter, CDOM, and inorganic sediments diminish the amount of light available for photosynthetic activity causing the depth of light penetration to differ dramatically between oceanic and coastal waters (Fig. 3a). In open ocean waters with relatively low phytoplankton, the blue-green wavelengths penetrate deeper in the water column. In contrast, high concentrations of both suspended particulate (phytoplankton and sediments) and dissolved matter strongly absorb the blue-green wavelengths in coastal waters thereby restricting penetration in deeper waters. The longer red wavelengths, however, are quickly absorbed by water molecules in near surface waters irrespective of the water optical type (Fig. 3b). In estuarine and fjordal ecosystems, with different fresh and saltwater mixing zones, the euphotic depth reduces gradually with increase in turbidity from the outer (downstream) to inner region (upstream) (Mascarenhas et al. 2017). It is in the euphotic zone, that the majority of primary production takes place.

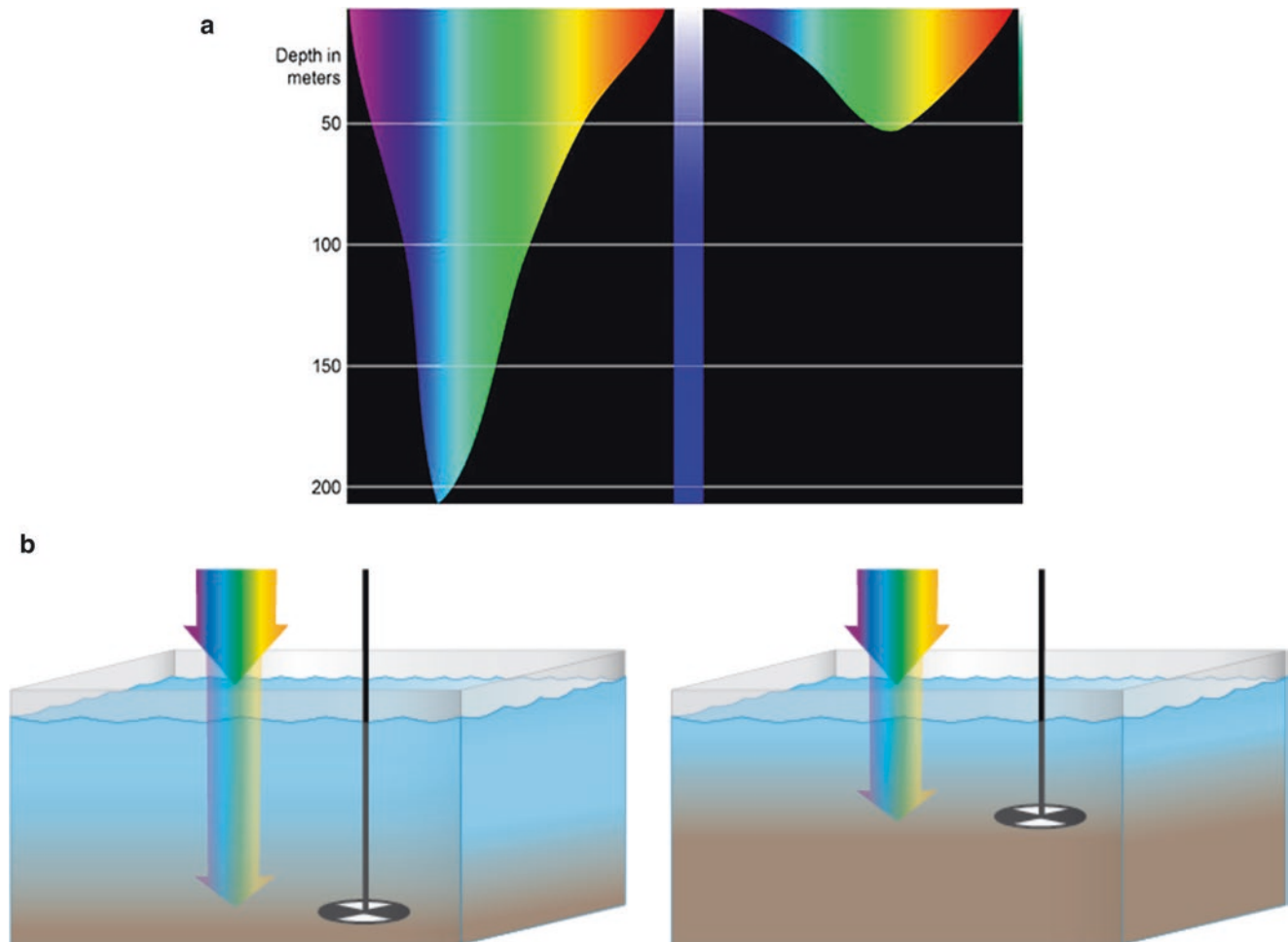


Fig. 3 Penetration of light underwater. (a) Spectral attenuation of visible light wavelengths (400–700 nm) in open and coastal waters. (Image courtesy of Kyle Carothers, NOAA-OE) (<http://oceanexplorer.noaa.gov/explorations/04deepscope/background/deeplight/media/diagram3.html>). (b) Light attenuation in clear (open) and turbid (coastal) waters. Low concentration of OACs allows deeper light penetration in open

ocean waters, while higher concentrations limit light penetration in turbid coastal waters. Measured with a Secchi disk (the black and white disk), the extent of light penetration, referred to as the Secchi disk depth, is an index of water clarity. (Courtesy of the Integration and Application Network, University of Maryland Center for Environmental Science (ian.umces.edu/symbols/))

Optical Classification of Water Types

Natural waters vary highly in their composition and thus also in the extent to which they transmit light underwater. Thus, oceanographers introduced ocean classification schemes based on the optical properties of water. The classification provided a broad indication of the water optical character. Jerlov first attempted to classify open ocean waters into 5 (I, IA, IB, II and III) and coastal waters into 9 different optical water types (numbered from 1 to 9) based on spectral light transmission curves (Jerlov 1976). Morel and Prieur (1977) subsequently introduced the Case 1 (optical properties dominated by phytoplankton and covarying material) and Case 2 (optical properties dominated by suspended sediments and

CDOM that vary independently of phytoplankton) classification schemes (based on the shape of reflectance spectra, Fig. 2).

Nature of Light and Light from the Sun

Light consists of numerous localized packets of electromagnetic energy, called photons moving with a velocity of $2.998 \times 10^8 \text{ ms}^{-1}$ in vacuum. Each photon carries a linear and an angular momentum. In addition, they also have an associated wavelength and frequency. Thus, photons exhibit both particle and wave nature and both aspects are fundamental for a proper understanding of light. Energy of a photon is

inversely proportional to its wavelength. That means shorter wavelengths possess more energy than the longer (Watson and Zielinski 2013).

How Is Radiation Measured?

In ocean (and also in freshwater ecosystems) optics, radiant energy is measured using two classes of light detectors: thermal and quantum. Thermal detectors (thermometers, thermocouples, bolometers, and pyranometers) absorb radiant energy and convert it into heat energy, wherein the detector responds to consequent changes in temperature of the absorbing medium. Quantum detectors (photographic films, photovoltaic, photoconductive, and photoemissive) react directly to the number of incident photons and not on the cumulative energy of the photons (Mobley 1994; Cunningham and McKee 2013).

Spectral radiance (unit: $\text{W sr}^{-1} \text{m}^{-2} \text{nm}^{-1}$) is the fundamental radiometric quantity of interest in aquatic optics. It is the radiant flux emitted, reflected, transmitted, or absorbed by a given surface, per unit solid angle per unit projected area. It describes the spatial, temporal, directional, and spectral structure of light. However, full radiance distributions are difficult to measure and assimilate. Therefore, quantities such as total scalar irradiance ($\text{W m}^{-2} \text{nm}^{-1}$), downward and upward (planar and scalar) irradiances are obtained by integrating radiances over defined intervals of solid angle. Profiling radiometer assemblies enable precise descriptions of radiative transfer in natural waters (Moore et al. 2009).

Reflectance (Fig. 2), an important AOP fundamental to remote sensing of the oceans, is computed from the above mentioned radiance and irradiance measurements. Earlier, ocean color remote sensing scientists used irradiance reflectance (the ratio of upwelling irradiance to downwelling irradiance) to develop algorithms for IOPs and other ocean parameter retrievals (Morel and Prieur 1977). However, recently, remote sensing reflectance (ratio of upwelling radiance to downwelling irradiance, measured just above the water surface) is more preferred by optical oceanographers (O'Reilly et al. 1998), as it is less sensitive to conditions such as sun angle and sky conditions. Radiative transfer studies relate water AOPs to IOPs.

Optical Tools

Optical oceanography relies strongly on field observations. Although the use of optics in the study of oceans dates back to ancient times, advances in optical technol-

ogy have played a crucial role in improving our understanding and exploration of the aquatic environments via means of imaging, vision, and sensing. Some of the earliest ocean color measurements were those of Secchi disc depth using a Secchi disk (Fig. 3b) named after the nineteenth century priest and astronomer Pietro Angelo Secchi aboard the papal yacht L'Immacolata Concezione to determine water transparency (Wernand 2010). These measurements were made using white discs of 0.4–3.75 m diameter to measure ocean clarity. Observations of light penetration depth were also made during Britain's 1872–1876 HMS Challenger expedition (Wernand 2013). The depth is determined by lowering the disc in water until it disappears from view.

In 1887, Francois Alphonse Forel introduced his ocean color comparator scale ranging from blue to green for identification of ocean color, later extended by Willie Ule from green to brown. Referred to as the Forel-Ule scale, it is well known and most commonly used in oceanography and limnology to determine color of natural waters. Wernand and van der Woerd (2010) proposed a reintroduction of the scale to expand the historical datasets and facilitate correlation with recent satellite ocean color observations. The scale is well characterized and stable ensuring coherent and well-calibrated datasets. Such simple methods have enabled participation from citizens through a number of citizen science projects such as the citclops (<http://www.citclops.eu/>) and eye on water (<http://eyeonwater.org/>) across Europe and beyond (Busch et al. 2016).

Optical sensors measure interaction of light (via absorption and scattering) with water constituents and thereby enable an assessment of the variability in water optical properties in relation to the observed OAC concentrations (Zielinski et al. 2009; Busch et al. 2013). Such observations are fundamental in the establishments of bio-optical models that relate OACs to their optical properties. Via methods of bio-optical inversion, these models enable determination of bio-geo-chemical parameters from remotely sensed signals (see section “Why do we use satellite measurements?”). Commonly used measurements of ocean color parameters include those of light transmission, absorption, scattering, fluorescence, and radiance distribution via methods of spectrophotometry, fluorometry, and radiometry respectively (Dickey et al. 2011). Sensors with selective membranes have enabled additional in situ monitoring of parameters like nutrients, dissolved oxygen, and carbon dioxide (Moore et al. 2009). However, field observations are limited in space and time and thereby lack regular or repeated global coverage. Therefore, satellite missions, which began monitoring the Earth in the 1960s, play an essential role by remotely

monitoring the global oceans and providing oceanographers with repeated synoptic coverage.

The next section of the chapter introduces the topic of satellite remote sensing of ocean color. It discusses briefly the developments in ocean color remote sensing over the last few decades, the challenges and processes involved and its applications.

Space-Borne Remote Sensing

Therese Keck

Why Do We Use Satellite Measurements?

Remote sensing is a technique describing properties of an object without having physical contact. Human eyes are sensible to the solar electro-magnetic spectrum from 400 to 700 nm ranging from violet to red (visible spectrum, VIS). Similar to the cones in our eyes, which detect different “colors”, water color measurement instruments are designed mostly within the optical spectrum in the visible and near-infra-red from 380 to 800 nm. Beyond these borders, water is strongly absorbing and the instruments receive no signal anymore. A monochromatic measurement may contain information about specific properties and a combination of certain bands can result, for instance, in an RGB image. Most of the instruments measure in a passive way by receiving reflected and back-scattered light from the water.

Generally, one of the most common questions in satellite remote sensing is “Why do we spend so much effort in converting electro-magnetic signals sensed with expensive and complex instruments which are far away in space”? Indeed, in situ and field measurements directly offer properties of the observed matter (e.g., algae content, temperature). Similar results from remote sensing require planning and operation of expensive sensors and their platforms as well as sophisticated algorithms to retrieve physical “products” (e.g., chlorophyll *a* concentration, water vapor content, temperature) from the satellite sensor signals. Nevertheless, the advantage is a relatively high and continuous spatial and temporal coverage of the entire globe.

For example, in Lake Erie (Fig. 4) at the border of Canada and the United States, large algae blooms appear every summer that can vary quickly in spatial and temporal dimension (Rowe et al. 2016). Harmful algae blooms (HABs) have a strong impact on the environment and are toxic to animals and humans. Satellite remote sensing enables us to investigate such events without being at the location or taking in situ samples. Therefore, measurements from even hardly or seldom reachable areas such as the open ocean or at high latitudes can be provided. Analyzing satellite sensor images,



Fig. 4 The western Lake Erie at the border of Canada and U.S. is known for extreme algae blooms. The OLCI RGB image shows a large bloom from 15 September 2017. (OLCI data provided from Copernicus/Eumetsat, RGB image produced with the freely available software SNAP (<http://step.esa.int/main/toolboxes/snap/>))

information about the spatial extent, location, and chlorophyll concentration are retrieved alongside other parameters. These data can be used to create climatologies and warnings.

Additionally, it is possible to detect a pattern’s temporal and spatial variability because satellites revisit the same geographic area every few days (e.g., the polar-orbiting satellites Terra and Aqua have a revisiting time of 1–2 days) or scan the area every few minutes (e.g., the geostationary Meteosat Second Generation MSG-10; EUMETSAT 2017). We are able to observe the atmosphere, the Earth’s surface, and the waters with space-borne remote sensing since more than 50 years on a daily to weekly base in a reasonable spatial resolution ranging from a few meters to several kilometers covering the entire earth. However, there is also remote sensing on Earth conducted in the field (e.g., on ships or at the Aeronautic Robotic Network (AERONET) stations) or in the air with instruments mounted on planes.

The knowledge of short- and long-term variability in the oceans and their constituents measured by remote sensing techniques serves as an important resource in oceanographic science. Since the 1960s, space-borne remote sensing supports human needs. “Satellite product users” (e.g., governmental administrations, environmental agencies, or scientific institutions) use “satellite products” to monitor freshwater

pools and to warn against pollution. Both play an important role for health and the environment.

The knowledge of the water constituents allows the prediction of fishing grounds and thereby providing economic benefits and sustainable exploitation of the oceans. In the case of natural disasters, satellite imagery provides a quick analysis of the extent and the impact finding quick ways for evacuation and first aid.

For example, the people in Cape Town, South Africa, suffer from severe drought since 2017 ongoing until now and the fresh water supply is strongly restricted since the beginning of 2018 due to a decrease of the largest reservoir, the Theewaterskloof Dam, to around 13% of its average capacity (A. Voiland, 2018-01-30, <https://earthobservatory.nasa.gov/IOTD/view.php?id=91649>, accessed 09 February 2018).

Environmental changes are observed by the variation in the constituents, the water extent, or the water level. Satellite images show erosion changes along coastlines or the growth of islands. Tracking phytoplankton supports fisheries, the transportation industry, and tourism industry identifying regions of high fish content (Moreira and Pires 2016), which they can either systematically avoid or locate. In order to warn against the toxicity of the HABs, governmental institutes are interested in identifying and tracking phytoplankton using remote sensing (Schaeffer et al. 2015).

The water availability and the water cycle play an important role in climate change. Climate models benefit from an improved understanding of changes and mechanisms analyzed from data retrieved from satellite remote sensing. Additionally, performing photosynthesis, phytoplankton is part of the carbon cycle and consume carbon dioxide, which is a major contributing agent in the frame of global warming. Field et al. (1998) reported that around 47% of the total net primary production is performed in marine ecosystems. Thus, it is of high importance to retrieve and understand the variability of the water constituents on all available temporal and spatial scales which already can almost be covered by remote sensing.

Overview of Technical Details

Platforms

The sensors that measure signals from the Earth's atmosphere, waters and land surfaces are mounted on satellite platforms. Each satellite flies in a specific orbit around the Earth and is loaded with power supplies, navigation tools, and support systems for the instruments. Generally, the most common satellite orbits are geostationary or polar-orbiting, which leads to differences in spatio-temporal resolutions. Geostationary satellites continuously monitor specified geographical locations above the Earth's surface in height of approximately 36,000 km. Therefore, they cannot cover the complete globe. For example, the Geostationary Ocean

Color Imager GOCI onboard the Communication Ocean and Meteorological Satellite 1 (COMS) captures images over Korean waters eight times a day (Ryu et al. 2012). Usually, television and communication satellites operate in this orbit due to the stable location.

Polar-orbiting satellites circle around the globe in approximately 100 min at a height of about 700–800 km. Their sensors are capable to cover the entire surface of the earth. The time to receive a full coverage depends on the sensor's swath (the scanning line or area on the ground) and can last from 2 to several days. The sensor Moderate Resolution Imaging Spectrometer (MODIS) onboard the platforms Aqua and Terra has a revisiting time of less than 3 days due to its large swath of 2330 km (Xiong et al. 2005). Polar-orbiting satellites are usually sun-synchronous: They cross the equator at the same local time (LT). Aqua passes the equator from South to North (ascending node) at 1:30 p.m. LT and Terra has an equator-crossing time of 10:30 a.m. LT in a descending node (Xiong et al. 2005). Figure 5a illustrates the product chlorophyll *a* calculated from MODIS/Terra for all available orbits for 2017-07-28.

Instruments

The measurement sensors or instruments are installed onboard the platform. There are two main measurement techniques. MODIS is a whiskbroom scanner, which oscillates across the satellite flight direction. Subsequently, it scans a part of the swath area from one side to the other and backwards while the satellite continues moving (Xiong et al. 2005). A sensor with a pushbroom measuring technique does not rotate: The whole swath width is scanned at once and pushed forward with the satellite flight direction and movement. The Medium Resolution Imaging Spectrometer MERIS onboard the Environmental Satellite (Envisat) is a prominent example (ESA 2006).

Most of the remote sensing instruments in space have multiple measuring bands or channels to detect a certain spectral range of light and its intensity. Mainly, a channel is defined by its central wavelength and the band width described by an individual response function. The function determines the ability of a band to detect a specific part of the electro-magnetic spectrum. For instance, the MODIS band 1 ranges from 620–670 nm detecting all photons within this wavelength range (Xiong et al. 2005). The response function defines how much of an infinitesimal wavelength interval contributes to the finally measured signal at this band. Chlorophyll *a* exhibits interesting features with an increase in absorption towards 670 nm in this spectral range (Bricaud et al. 1998). Using measuring bands with a large band width leads to a loss of specific spectral features which particularly reduces the information quality in water bodies. Therefore, it is important to carefully specify the spectral settings of a channel depending on the sensor's objective.

There are spectrometers with a higher spectral resolution than MERIS or MODIS. For example, the latest space-borne

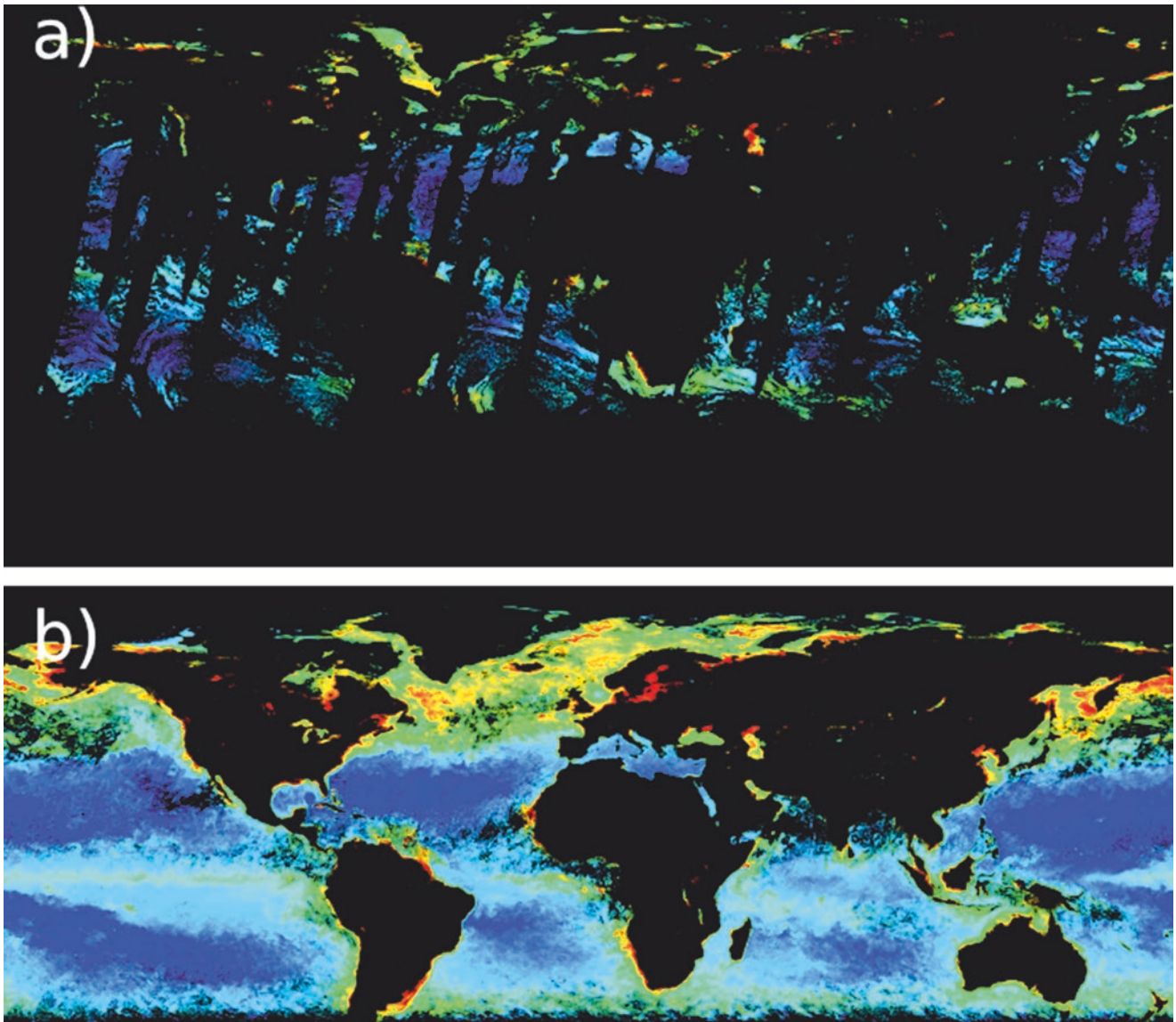


Fig. 5 Global coverage of the MODIS (Terra) Level-3 product Chlorophyll *a* concentration (OCI-Algorithm) on a daily base (28 July 2017) and monthly mean for June 2017. (Pictures provided by Ocean

Biology Processing Group/NASA, downloaded from <https://ocean-color.gsfc.nasa.gov/cgi/13> (29 July 2017))

sensors HICO (Hyperspectral Imager for the Coastal Ocean) or the future HSI (Hyperspectral Imager) onboard EnMAP (The Environmental Mapping and Analysis Program) are hyperspectral sensors exhibiting measurement bands every 5–10 nm, which enables us to investigate even narrow spectral features (e.g., the phytoplankton peak near 683 nm).

Measurement

The satellites operate at a height where the atmosphere is already extremely thin and, therefore, negligible. Hence, we distinguish between at-sensor-measurements at top of the atmosphere (TOA) and bottom of atmosphere (BOA) measurements which are back-calculated from the TOA measurements. The TOA measurement signal contains

information about the atmosphere and the underlying water body or land surface. Depending on the atmospheric composition (gas mixtures, aerosols, clouds), the intensity reduces by absorption and scattering in the incident direction. It can also increase if diffuse sky light scatters in the direction of the incoming solar radiation.

At the water surface, the incident radiation is partly reflected in the atmosphere and the other part penetrates the water. Depending on the water conditions defined by the water properties and the constituents, most of the radiation is absorbed or scattered. A little part is scattered backwards and leaves the water again. The amount of water-leaving photons depends on the atmospheric and water conditions and the radiation has to pass the atmosphere again to approach at the

sensors at top at the atmosphere. Mathematically, the measured signal is a function of all conditions and constituents of the atmosphere and the water. We can access these parameters by inversion (exemplary, see inversion techniques described in Rodgers 2000). Generally, the retrieved TOA signal contains approximately 90% atmospheric and 10% oceanic information.

Additionally, the TOA measurement changes with the spectrum and the viewing geometry. As outlined beforehand, in the near infrared we expect a very low or no signal above (clear) water bodies due to the strong absorptive properties of waters beyond 750 nm but a high response in the blue visible range. Most of the optical instruments have a nadir viewing geometry where the measurement sensor looks directly downwards. An off-nadir measurement with a viewing zenith angle (VZA) greater than 0° from the normal axis between satellite and surface increases the path between the location of the water-leaving radiation and the sensor. The signal can increase by diffuse scattering in the atmosphere and/or attenuates due to more opportunities for absorption and scattering by molecules and particles.

The main natural obstacles (along others) in optical remote sensing are clouds, sunglint, and the interfering atmosphere. Clouds appear thick and white to the human eyes and also to optical sensors. In different wavelengths regimes, for example for microwave measurements, clouds are transparent and the sensors can measure the underlying surface. Usually, microwave instruments are used for the detection of sea surface temperature, surface height or land applications. For optical measurements, certain algorithms (“cloud masks”) exclude pixels with expected cloud coverage. Sunglint occurs at smooth and highly reflective surfaces such as water or fresh snow if the solar light is directly reflected into the sensor. The bright reflection usually oversaturates a sensor’s measurement capability and also contains very low or no information about the water body. However, a change in the viewing geometry reduces or even avoids the measurement of sunglint.

The measured TOA radiation has to pass the atmosphere, which highly changes the received signal that leaves the water. The measurement can be “back-calculated” to a BOA-measurement, which is ideally equal to the water-leaving signal. Therefore, it is necessary to estimate the influence of the atmosphere on the TOA-signal by proxies and additional measurements. Using the estimation, the signal can be corrected for the atmosphere (“Atmospheric Correction”).

Selected Sensors for Water Remote Sensing

Historically, scientific Earth observation started in the late 1950s to support weather forecasts and to analyze weather phenomena. In the following, we present some selected sensors that have or had the main mission to observe water bodies. Therefore, each sensor’s bands were carefully chosen for

water applications. However, they are also used above land and most of the introduced sensors also have land and atmospheric missions.

The Coastal Zone Color Scanner (CZCS) onboard the US-platform NIMBUS-7, operational from 1978 to 1987, was one of the first satellite sensors mainly designed to observe the oceans. The CZCS measurements were a first step towards global mapping of chlorophyll *a* concentration and the impact of the oceans on the carbon cycle. In 1996, the Sea-viewing Wide Field-of-view Sensor (SeaWiFS) onboard Seastar began sensing the ocean in eight channels within 400 nm to 900 nm. SeaWiFS operated until 2010 and was slightly tilted to avoid sun glint. MODIS, introduced in section “[Instruments](#)”, is mounted on board the satellites Aqua and Terra operating from 1999 and 2002, respectively, until present time. The Medium Resolution Imaging Spectrometer MERIS was one of 11 instruments onboard the Environmental Satellite Envisat that operated from 2002 until a technical platform failure in 2012. MERIS supported the chlorophyll *a* fluorescence investigation with a band at 681 nm nearly to 683 nm where the fluorescence peaks and some bands usable for chlorophyll *a* algorithms (ESA 2006).

The Ocean and Land Color Imager (OLCI) on board Sentinel-3 continues the heritage of MERIS with 6 additional bands (ESA 2013). Sentinel-3A was launched in 2016 and Sentinel-3B is planned for 2018 (<https://earth.esa.int/web/guest/missions/esa-eo-missions/sentinel-3>, 29 July 2017). Hyperspectral imagers usable for water measurements are the Hyperspectral Imager for the Coastal Ocean (HICO) installed on the International Space Station (ISS) and the Hyperspectral Imager (HSI) onboard EnMAP. HICO operated from 2008 to 2014 (<http://hico.coas.oregonstate.edu/>, 29 July 2017-07-29) and EnMAP is planned for launch in 2019 (<http://www.enmap.org/>).

Using Remote Sensing Measurements

Preprocessing

Before the space-borne measurements are available for the user, they are usually preprocessed. The state of processing is defined by its level. The processing is mostly done by the operating space agency and, hence, the expressions may sometimes vary slightly and the agencies may not provide all levels for all sensors. Referring to Martin (2014) the levels (L) are briefly introduced:

Level 0 data sets contain the raw measurements without any correction besides measurement or transfer artifacts.

Level 1 data sets contain temporal and spatial information.

Level 1B data provide measurements converted to a radiometric unit (e.g., radiance).

Level 2 data sets contain physical parameters calculated from L1B data (e.g., sea surface temperature). L2 data require the application of multiple channels, land-sea-masks and cloud masks, and usually an atmospheric correction that accounts for the influence of the atmosphere on the signal.

Sometimes, Levels 3 products are available for specific locations or a specific gridding. They may also contain temporally merged products, e.g., monthly means, to reduce data gaps due to clouds or other obstacles. Figure 5a illustrates daily Chlorophyll *a* product from 28 July 2017 and a monthly mean for the month of June 2017 is given in Fig. 5b. Level 4 data may incorporate match-up data of in situ and field measurements. In oceanic applications, the atmospheric correction for the Level 2 data is mainly applied to convert the TOA measurements into values that would have been measured if the atmosphere were absent. There is a wide range of applications and algorithms that can conduct atmospheric corrections.

Applications

All levels are usually provided in a scientific binary data format and are mostly available for free (e.g., MODIS data) or on request for scientific purposes. Oceanic remote sensing data can be downloaded via the following selected webpages:

- <https://oceancolor.gsfc.nasa.gov/> for SeaWiFS, MODIS, MERIS, CZCS, and others. They provide Chlorophyll-concentration, sea surface temperature, and a quasi-RGB image per orbit or on a temporal averaged base.
- <https://scihub.copernicus.eu/s3/#/home> for OLCI data as Level 1 or Level 2

EumetView provides a quick access to OLCI data with orbital RGB images (access via <http://eumetview.eumetsat.int/mapviewer/>). The RGB image can be downloaded. The WorldView page for the MODIS measurements (<https://worldview.earthdata.nasa.gov/>) supports RGB images, reflectance, and several layers (e.g., sea ice and chlorophyll concentration) for an easy overview of the entire globe. Both views provide images in near-real time.

The free software SNAP (download via <http://step.esa.int/main/toolboxes/snap/>) by ESA is a useful tool for statistical analyses of satellite data and display results per band or as RGB image (see Figs. 4 and 6). For some sensors, it provides atmospheric corrections, conversion to a higher level and generation of products like chlorophyll concentration.

For example, the two band ratio “blue-green-ratio” gives a first estimation of the amount of algae and chlorophyll, respectively, in the ocean in arbitrary units (Martin 2014). In clear waters, the maximum reflectance is located in the blue part of the visible spectrum. The peak shifts to the green regime in the presence of phytoplankton. The blue-green-

ratio $BG = \text{“blue channel”}/\text{“green channel”} = R(440 \text{ nm})/R(555 \text{ nm})$ compares these two extremes. A higher blue-green-ratio indicates a “more blue” water and we expect low or no algal content. Unfortunately, this ratio is easily disturbed by additional substances (CDOM, sediments) that change the shape of a reflectance spectrum. Therefore, this ratio is only applicable for a first guess in clear waters with phytoplankton dominance.

Bio-optical Models

Bio-optical models link optical measurements of reflectance or radiance and biological parameters like chlorophyll *a* concentration, water quality, euphotic depth, and others. These biogeochemical variables are a main interest of the end-users who want to decide or analyze specific issues. Depending on the observed water, the complexity of a bio-optical model can vary from a ratio to an extensive non-linear function. Morel and Prieur (1977) introduced optically simple waters, which only contain phytoplankton (case-1) and optically complex waters (case-2). Exemplarily in case-1 waters, several chlorophyll *a* concentration algorithms are based on blue-green ratios (BGs). BG is the relation between a “green” and “blue” measurement band in the VIS providing a qualitative estimate of the relative presence of phytoplankton.

According to Martin (2014), the MODIS Ocean-Color-3-band-Algorithm OC3M is an empirical relation between the maximal ratio of some blue-green ratios from measured reflectance and chlorophyll *a* [mg m^{-3}] measurements:

$$R_L = \log_{10} \left(\max \left[R_{rs} (443\text{nm}, 488\text{nm}) / R_{rs} (551\text{nm}) \right] \right)$$

$$\log_{10} (\text{Chla}) = 0.2424 - 2.742 * R_L + 1.802 * R_L^2 + 0.002R_L^3 - 1.228R_L^4$$

Where R_{rs} refers to remote sensing reflectance, R_L to the maximal ratio and Chla to chlorophyll *a* concentration.

There is a wide range of “OC” algorithms depending on the instrument and the degree of the polynomial. Bio-optical models also can describe the spectral shape of IOPs based on only a few measurements, for example,

$$a_{\text{CDOM}} = a_{\text{CDOM}}(440) * \exp(-S * (\lambda - 440))$$

where a_{CDOM} refers to absorption by CDOM, and S to the slope of the absorption spectra. CDOM absorption (m^{-1}) exponentially decreases with longer wavelengths and a bio-optical model for spectral CDOM is often based on a measurement at approximately 440 nm. The equations for a_{cdom} and phytoplankton absorption (a_{ph}) are commonly used models to describe CDOM in case-2 waters and phytoplankton absorption in case-1 waters (Gilerson et al. 2008; Brewin et al. 2011; McKee et al. 2014). Usually, the shape factor S

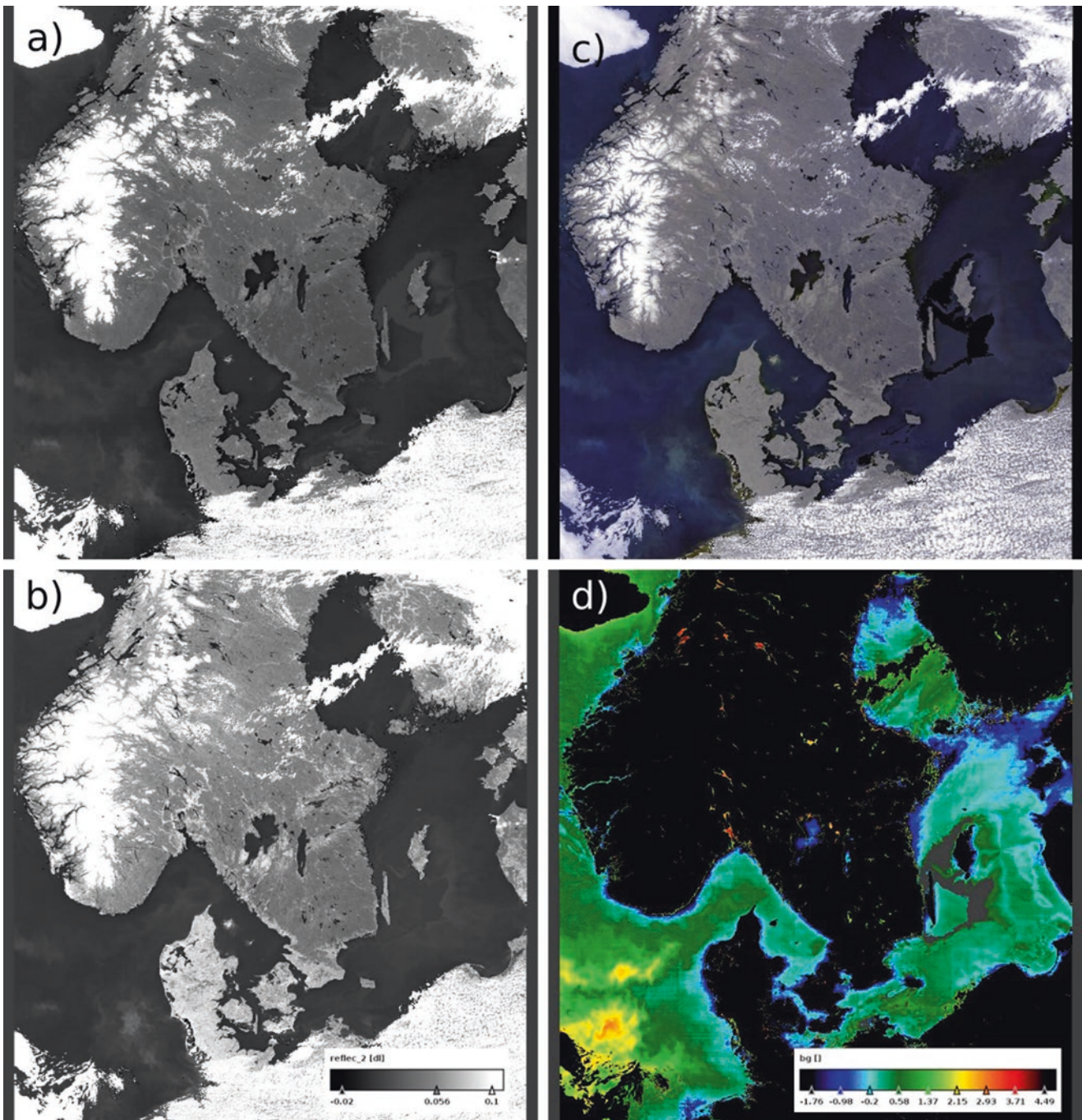


Fig. 6 MERIS captured the North Sea and Baltic Sea on 06 June 2008. (a) and (b) Level-2 reflectance for the channels 442 nm and 560 nm, respectively, share the color bar from panel. (c) RGB image calculated with several bands. (d) blue-green-ratio between the 442 nm and the

560 nm band. (Produced with the freely available software SNAP (<http://step.esa.int/main/toolboxes/snap/>) and the MERIS data are provided from the Ocean Biology Processing Group/NASA)

of the exponential decrease ranges from 0.005 nm^{-1} to 0.031 nm^{-1} (Brewin et al. 2015; Bricaud et al. 2012; Chen et al. 2017) and the reference is usually set to an available blue wavelength (440 nm).

In case-2 waters, Stedmon et al. (2000) and Kowalczyk et al. (2006) analyzed CDOM in Danish coastal waters and

in the Baltic Sea and found a dependency on the origination of CDOM and seasonal stratification, respectively. This shows the complexity of case-2 waters. Bricaud et al. (1995) and Bricaud et al. (1998) found an empirical equation for chlorophyll concentration and absorption with spectral dependent coefficients A [$\text{m}^3 \text{ mg}^{-1}$] and B [dl] in open

oceans. Therefore, the model is mainly valid for case-1 waters:

$$a_{ph}(\lambda) = A(\lambda) * chl a^{1-B(\lambda)}$$

where a_{ph} refers to phytoplankton absorption, chl a is the chlorophyll a concentrations, A and B wavelength dependent parameters. Retrieving results from this bio-optical model, the chlorophyll concentration is needed. Therefore, the model is highly dependent on accurate measurement results of chlorophyll, which can be complicated in case-2 waters due to the possible presence of additional water constituents such as CDOM.

Alongside the relations between optical properties and biogeochemical constituents and the spectral expression of IOPs, bio-optical models can also relate different IOPs to each other. For instance, the degradation products of phytoplankton have similar optical properties to CDOM and the amount increases with increasing chlorophyll a (e.g., Bricaud et al. 2012). Thus, there is a natural correlation of both absorption coefficients. Based on data of the North Sea merged from Nechad et al. (2015), a bio-optical model relating CDOM and a_{ph440} yields for 440 nm.

$$cdom(440nm) = 0.24 * a_{ph}(440nm)^{0.43}$$

There are also bio-optical models related to scattering of non-algal particles of phytoplankton. However, estimating or measuring scattering coefficients is more difficult than absorption coefficients due to a high dependence on the viewing angle and the anisotropic behavior of the scattering phase function constraining the direction of the scattered light (Petzold 1972).

Pure water absorption and scattering coefficients have been measured and analyzed in laboratory experiments and, for instance, are provided by Pope and Fry (1997). Bio-optical models are a highly important part in modeling of water bodies and the simulations and prediction can differ significantly due to the choice of the models. There are a wide range of bio-optical models that can be found in literature due to the difficulty in measurement (e.g., measurement technique and site selection) and various empirical and statistical relations and concepts.

Conclusions and Outlook

Ocean color is an index of ecosystem health. Changes in ocean color indicate changes in its optical constituents that contribute to ocean color. Regular monitoring of these changes is important as it allows the health of ecosystems to be kept in check. Advances in optical methodologies have greatly improved our understanding of the oceanic environ-

ment. However, the ever increasing effects of anthropogenic influence and climate change, repeated spatial and temporal coverage is of utmost relevance. Satellite remote sensing, therefore, plays an important role by providing opportunities of global monitoring of the vast and dynamic oceanic ecosystem. Being recognized as an essential climate variable (ECV) ocean color is monitored as part of the climate change initiative (CCI) project of the European Space Agency (ESA) in the global climate observing system (GCOS).

However, accurate interpretation of the remotely sensed signal is challenging and requires good estimation of atmospheric corrections. Furthermore, the complexities are amplified in the complex case-2 waters owing to the contribution of non-varying optical components like CDOM and inorganic suspended sediments. Development of region specific algorithms therefore becomes necessary. Hence, in situ observations still continue to play an important role in bio-optical algorithm development and validation purposes. Moreover, satellite observations of the surface ocean in combination with bio-optical algorithms (derived from in situ autonomous profiling systems, e.g., buoys, floats) are being incorporated into the development of 3D bio-optical ocean models with potential applications in physics and biogeochemistry of the dynamic environment at a number of relevant scales.

For further reading we recommend ‘Ocean optics web book’ (<http://www.oceanopticsbook.info/>) and the ‘IOCCG Report Series’ (<http://ioccg.org/what-we-do/ioccg-publications/ioccg-reports/>).

Acknowledgments Authors are extremely thankful to the reviewer for providing helpful comments, which greatly improved the chapter. The chapter contains modified Copernicus Sentinel data (2017) and Ocean Biology Processing Group (OBPG) data products and images.

Appendix

This article is related to the YOUMARES 8 conference session no. 7: “Ocean Optics and Ocean Color Remote Sensing”. The original Call for Abstracts and the abstracts of the presentations within this session can be found in the appendix “Conference Sessions and Abstracts”, chapter “3 Ocean Optics and Ocean Color Remote Sensing”, of this book.

References

- Aksnes DL, Nejstgaard J, Sædberg E et al (2004) Optical control of fish and zooplankton populations. *Limnol Oceanogr* 49:233–238. <https://doi.org/10.4319/lo.2004.49.1.0233>
- Aksnes DL, Dupont N, Staby A et al (2009) Coastal water darkening and implications for mesopelagic regime shifts in Norwegian fjords. *Mar Ecol Prog Ser* 384:39–49

- Binding CE, Jerome JH, Bukata RP et al (2008) Spectral absorption properties of dissolved and particulate matter in Lake Erie. *Remote Sens Environ* 112(4):1702–1711
- Brewin RJ, Hardman-Mountford NJ, Lavender SJ et al (2011) An inter-comparison of bio-optical techniques for detecting dominant phytoplankton size class from satellite remote sensing. *Remote Sens Environ* 115(2):325–339
- Brewin RJ, Raitos DE, Dall’Olmo G et al (2015) Regional ocean-colour chlorophyll algorithms for the Red Sea. *Remote Sens Environ* 165:64–85
- Bricaud A, Babin M, Morel A et al (1995) Variability in the chlorophyll-specific absorption coefficients of natural phytoplankton: analysis and parameterization. *J Geophys Res* 100(C7):13321–13332
- Bricaud A, Morel A, Babin M et al (1998) Variations of light absorption by suspended particles with chlorophyll *a* concentration in oceanic (case 1) waters: analysis and implications for bio-optical models. *J Geophys Res* 103(C13):31033–31044
- Bricaud A, Ciotti A, Gentili B (2012) Spatial-temporal variations in phytoplankton size and colored detrital matter absorption at global and regional scales, as derived from twelve years of SeaWiFS data (1998–2009). *Global Biogeochem Cycles* 26:GB1010
- Busch JA, Zielinski O, Cembella AD (2013) 8 – optical assessment of harmful algal blooms (HABs). In: Watson J, Zielinski O (eds) *Subsea optics and imaging*. Woodhead Publishing, Oxford, pp 171–214e. <https://doi.org/10.1533/9780857093523.2.171>
- Busch JA, Price I, Jeansou E, Zielinski O, van der Woerd HJ (2016) Citizens and satellites: assessment of phytoplankton dynamics in a NW Mediterranean aquaculture zone. *Int J Appl Earth Obs Geoinf* 47:40–49
- Chang GC, Dickey TD (2004) Coastal ocean optical influences on solar transmission and radiant heating rate. *J Geophys Res* 109:C01020
- Chen J, He X, Zhou B, Pan D (2017) Deriving colored dissolved organic matter absorption coefficient from ocean color with a neural quasi-analytical algorithm. *J Geophys Res* 122:8543–8556
- Coble PG (2007) Marine optical biogeochemistry: the chemistry of ocean color. *Chem Rev* 107(2):402–418
- Cunningham A, McKee D (2013) 4 – Measurement of hyperspectral underwater light fields. In: Watson J, Zielinski O (eds) *Subsea optics and imaging*. Woodhead Publishing, Oxford, pp 83–97. <https://doi.org/10.1533/9780857093523.2.83>
- Dickey TD, Kattawar GW, Voss KJ (2011) Shedding new light on light in the ocean. *Phys Today* 64(4):44–49
- ESA (2006) Meris product handbook. URL http://envisat.esa.int/pub/ESA_DOC/ENVISAT/MERIS/
- ESA (2013) Sentinel-3 user handbook, Tech Rep. 1. URL <https://sentinel.esa.int>
- EUMETSAT (2017) MSG level 1.5 image data format description, Tech. Rep. 105-v8, Darmstadt. URL <https://www.eumetsat.int/web-site/home/Data/TechnicalDocuments/index.html>
- Field CB, Behrenfeld MJ, Randerson JT et al (1998) Primary production of the biosphere: integrating terrestrial and oceanic components. *Science* 281(5374):237–240
- Frank TM, Johnsen S, Cronin TW (2012) Light and vision in the deep-sea benthos: II. Vision in deep-sea crustaceans. *J Exp Biol* 215(19):3344–3353. <https://doi.org/10.1242/jeb.072033>
- Garaba SP, Voß D, Zielinski O (2014) Physical, bio-optical state and correlations in north-western European shelf seas. *Remote Sens* 6(6):5042–5066
- Gilerson A, Zhou J, Hlaing S et al (2008) Fluorescence component in the reflectance spectra from coastal waters. II. Performance of retrieval algorithms. *Opt Express* 16(4):2446–2460
- Gnanadesikan A, Emanuel K, Vecchi GA et al (2010) How ocean color can steer Pacific tropical cyclones. *Geophys Res Lett* 37:L18802
- Holinde L, Zielinski O (2016) Bio-optical characterization and light availability parameterization in Uummannaq Fjord and Vaigat–Disko Bay (West Greenland). *Ocean Sci* 12:117–128
- Jerlov NG (1976) *Marine optics*, Elsevier oceanography series 14. Elsevier Scientific Publishing Company, Amsterdam
- Kirk JT (1994) *Light and photosynthesis in aquatic ecosystems*. Cambridge University Press, Cambridge
- Kowalczyk P, Stedmon CA, Markager S (2006) Modeling absorption by CDOM in the Baltic Sea from season, salinity and chlorophyll. *Mar Chem* 101(1–2):1–11
- Martin S (2014) *An introduction to ocean remote sensing*. Cambridge University Press, Cambridge
- Mascarenhas V, Voß D, Wollschlaeger J et al (2017) Fjord light regime: bio-optical variability, absorption budget, and hyperspectral light availability in Sognefjord and Trondheimsfjord, Norway. *J Geophys Res* 122:3828–3847
- McKee D, Röttgers R, Neukermans G et al (2014) Impact of measurement uncertainties on determination of chlorophyll-specific absorption coefficient for marine phytoplankton. *J Geophys Res* 119:9013–9025
- Mobley CD (1994) *Light and water: radiative transfer in natural waters*. Academic, Dan Diego
- Moore C, Barnard A, Fietzek P et al (2009) Optical tools for ocean monitoring and research. *Ocean Sci* 5:661–684
- Moreira D, Pires JC (2016) Atmospheric CO₂ capture by algae: negative carbon dioxide emission path. *Bioresour Technol* 215:371–379
- Morel A, Prieur L (1977) Analysis of variations in ocean color. *Limnol Oceanogr* 22(4):709–722
- Nechad B, Ruddick K, Schroeder T et al (2015) CoastColour Round Robin data sets: a database to evaluate the performance of algorithms for the retrieval of water quality parameters in coastal waters. *Earth Syst Sci Data* 7(2):319–348
- O’Reilly JE, Maritorena S, Mitchell BG et al (1998) Ocean color chlorophyll algorithms for SeaWiFS. *J Geophys Res* 103:24937–24953
- Petzold TJ (1972) Volume scattering functions for selected ocean waters. *Scripps Institution of Oceanography, San Diego*
- Pope RM, Fry ES (1997) Absorption spectrum (380–700 nm) of pure water. II. Integrating cavity measurements. *Appl Opt* 36(33):8710–8723
- Rodgers CD (2000) *Inverse methods for atmospheric sounding: theory and practice*. World scientific, Singapore
- Rowe M, Anderson E, Wynne TT et al (2016) Vertical distribution of buoyant *Microcystis* blooms in a Lagrangian particle tracking model for short-term forecasts in Lake Erie. *J Geophys Res* 121:5296–5314
- Ryu J-H, Han H-J, Cho S et al (2012) Overview of geostationary ocean color imager (GOCI) and GOCI data processing system (GDPS). *Ocean Sci* 47(3):223–233
- Schaeffer BA, Loftin KA, Stumpf RP et al (2015) Agencies collaborate, develop a cyanobacteria assessment network. *EOS, Earth Space Sci News* 96. <https://doi.org/10.1029/2015EO038809>
- Stedmon C, Markager S, Kaas H (2000) Optical properties and signatures of chromophoric dissolved organic matter (CDOM) in Danish coastal waters. *Estuar Coast Shelf Sci* 51(2):267–278
- Watson J, Zielinski O (2013) *Subsea optics and imaging*. Woodhead Publishing, Oxford
- Wernand M (2010) On the history of the Secchi disc. *J Eur Opt Soc Rap Publ* 5:10013s

- Wernand MR (2013) 3 – The history of subsea optics. In: Watson J, Zielinski O (eds) *Subsea optics and imaging*. Woodhead Publishing, Oxford, pp 35–79. <https://doi.org/10.1533/9780857093523.1.35>
- Wernand M, van der Woerd HJ (2010) Spectral analysis of the Forel-Ule Ocean colour comparator scale. *J Eur Opt Soc Rap Publ* 5:10014s
- Xiong J, Toller G, Chiang V et al (2005) MODIS level 1B algorithm theoretical basis document, NASA MODIS characterization support team, Washington, DC
- Zielinski O, Busch JA, Cembella AD et al (2009) Detecting marine hazardous substances and organisms: sensors for pollutants, toxins, and pathogens. *Ocean Sci* 5:329–349

Open Access This chapter is licensed under the terms of the Creative Commons Attribution 4.0 International License (<http://creativecommons.org/licenses/by/4.0/>), which permits use, sharing, adaptation, distribution and reproduction in any medium or format, as long as you give appropriate credit to the original author(s) and the source, provide a link to the Creative Commons license and indicate if changes were made.



The images or other third party material in this chapter are included in the chapter's Creative Commons license, unless indicated otherwise in a credit line to the material. If material is not included in the chapter's Creative Commons license and your intended use is not permitted by statutory regulation or exceeds the permitted use, you will need to obtain permission directly from the copyright holder.